JOURNAL OF APPLIED ELECTROCHEMISTRY **26** (1996) 385–396

Study of a mechanism of hard gold electrodeposition

W. CHRZANOWSKI*, Y. G. LI, A. LASIA‡

Département de Chimie, Université de Sherbrooke, Sherbrooke, Québec, J1K 2R1, Canada

Received 9 November 1994; revised 21 June 1995

Electrodeposition of nickel hardened gold was studied from a proprietary bath (Renovel N). Linear sweep voltammetry (LSV), chronoamperometry and chronopotentiometry were employed and Tafel curves determined. LSV studies revealed formation of a current peak connected with the inhibition of the deposition reaction. In the hard gold bath Tafel curves are characterized by two slopes: $-0.47\,V\,dec.^{-1}$ between -0.5 and $-0.8\,V$ and $-0.19\,V\,dec.^{-1}$ at more negative potentials; in the soft gold bath (without Ni) these slopes are: $-0.35\,V\,dec.^{-1}$ and $-0.15\,V\,dec.^{-1}$, respectively. Current efficiency of hard gold plating in galvanostatic conditions was on the average 54–57%, depending more on current density than on the charge passed (thickness of the deposit). No influence of oxygen on the process was found. It was also found, that the bath must be activated before reproducible results are obtained.

1. Introduction

Electrodeposition of hard gold remains in the centre of interest of the electroplating industry because of its practical significance in the electronic industry [1–4]. So called 'hard gold' is, in fact, an alloy containing a small percentage of the hardening metal, usually nickel or cobalt [1–26], although use of other metals [5, 9] and additive-free gold [27–30] have also been reported. The main directions of the research in the field of gold plating are as follows:

(i) Testing different bath compositions and evaluating the influence of plating parameters to obtain high-speed plating, optimal throwing power, as well as the macroproperties (e.g., wearing resistance, hardness, porosity) and/or desired microstructure of the deposits [26, 31–33].
(ii) Testing new plating techniques, mainly those utilizing pulse current technique [7, 12, 14, 23, 24, 31, 32, 35] and laser enhanced electrodeposition [36].
(iii) Studying the kinetics of electrode processes [33, 37], including the electrocrystallization step [38, 39]. Some studies of electrocrystallization of gold are reported [35, 40], although only one refers to modelling of chronoamperometric transients (for soft gold electrodeposition) on the basis of nucleation and crystal growth theory [41].
(iv) Studies of side effects and byprocesses of different type which either shorten the bath lifetime or worsen the quality of the deposits [10, 11, 48, 49]. The latter may be influenced by contamination of the deposit with polymeric materials [50–53], carbon and carbonaceous materials [54–58], as well as by other factors [59–63].
(v) Assessment of different commercially available baths, as well as development of new baths with favourable parameters of plating and deposits [8, 10, 12, 31, 32, 40, 42–47, 52, 64].

Among the experimental techniques utilized in the above mentioned studies, the dominating group are classical electrochemical methods like linear sweep voltammetry (LSV), cyclic voltammetry (CV), chronoamperometry (CA) and chronopotentiometry (CP). Besides, one can expect electrochemical impedance spectroscopy [65] to play a more significant role in such studies. The electrochemical methods are usually coupled with appropriate analytical methods for measuring bath composition and its changes, deposit composition and its in-depth profile, as well as for the assessment of the deposit properties. These methods include wide scope of analytical techniques to discuss them in details, although, a group of microscopic techniques should be mentioned [8, 9, 18, 22, 31–36, 40, 41, 50, 52, 57–60, 64, 66]. Electrochemical studies were most often performed on flat electrodes with hydrodynamic conditions described only generally as 'agitation'. Rotating disc electrodes (RDE) [17, 33, 37], rotating cylinder electrodes [28, 48, 66] and specially designed electrode assemblies [6, 12, 26, 32, 35] have also been reported. It seems possible that wall-jet electrodes [68–70] will serve as a suitable physical model for studies of electrodeposition.

The aim of this paper is to present a study of the mechanism of nickel-hardened gold electrodeposition from commercial Renovel N bath. This bath belongs to a group of acidic baths (pH 4.4) utilizing $KAu(CN)_2$ as a source of gold. In the present paper we present the results and conclusions from the LSV, CA and CP experiments, as well as current efficiency measurements. More detailed considerations regarding the initial stages of nucleation and crystal growth will be published in further papers.

* On leave from the Technical University of Gdańsk, 80-952 Poland.
‡ Author to whom all correspondence should be addressed.

0021-891X

2. Experimental details

The bath under study consists of three major components: (1) the proprietary supporting electrolyte (Renovel N make-up solution, LeaRonal, Freeport, NY); (2) proprietary nickel containing solution, blue nickel complex (Renovel N nickel concentrate, LeaRonal); and (3) $KAu(CN)_2$ (SEL–REX, Enthone-OMI).

Four different solutions were prepared from bath components:

A, containing component 1 only;
B, containing components 1 and 2;
C, containing components 1 and 3 (soft gold plating bath);
D, containing all components (hard gold plating bath).

Each of the above listed solutions has been diluted after mixing of its components to the same final volume as the full bath (concentrations of particular components, if present, were the same in all solutions, Ni: 2.73×10^{-2} M and Au: 9.12×10^{-2} M). Deionized (DI) water (Barnstead, Nanopure) was used in all the experiments. The pH value of all solutions (A though D) was about 4.4. All other reagents and chemicals used were of analytical grade.

Potentiostat (models 273A or 263, EG&G Princeton Applied Research) controlled by IBM compatible microcomputer by means of PAR M270/250 Research Electrochemical Software and PAR Headstart Creative Electrochemistry Software was utilized in electrochemical experiments. Working RDEs used in this study were home-made with a gold RDE or AFAD03Au (Pine Instrument Company) electrode – both of 0.07 cm^2 geometric surface area and a platinum RDE of AFDD40Pt (Pine) type – 1 cm^2. The rotator was of AFASR type (Pine). Thermostated cell with cathodic compartment of ~250 ml and anodic compartment separated with Nafion® 117 (DuPont) membrane was used. The cathodic part was continuously purged with nitrogen (at least 2 h before experiments) unless stated otherwise. The anodic part was always filled with solution A. The working temperature was 60 °C. Counter electrodes were either platinum mesh, or graphite rod. The reference electrode was always SCE, which remained in contact with the solution via Luggin capillary. Solution resistance was measured by means of a.c. impedance spectroscopy and the curves were corrected for iR drop numerically.

The gold RDE was prepared for the measurements by polishing its surface on a rotating table (GP-60 Polisher, Leco Corp.) using Gamma Micropolish Alumina (Buehler) 1 μm and/or 0.05 μm, washing thoroughly, immersing in HNO_3 (1 : 1) for 10 s and, again, washing with deionized water. For the determination of current efficiency, the platinum RDE with electrodeposited gold was transferred into the stripping cell with 1 M HCl and the layer was stripped off under constant current conditions. The solution was then analysed by means of AAS spectrophotometer (Video 12 type, Instrumentation Laboratory) with gold hollow cathode lamp (Hamamatsu Photonics, Japan). To reduce any influences of the AAS measurements on the results, we performed the analyses of collected samples in a random order rather than as the samples were collected in respective series of deposition-stripping experiments.

To have the bath composition under control, regular checks of its gold and nickel contents were performed by means of AAS. Additionally, check procedure was established for the possible changes in the solution composition, due to the unknown factors, which can be generally described as bath ageing. This procedure was performed daily and it consisted of a LSV curve measurement at scan rate $v = 1\,mV\,s^{-1}$ and rotation rate 2600 rpm. In the cases when deviations from original and well established pattern were observed, the solution under study was discarded. The actual experimental error, expressed as a relative difference between two curves recorded over a span of days, under the same conditions, eventually varied from 1 to 5%, depending on the current range.

3. Results and discussion

3.1. *Preliminary experiments*

The potential range for LSV measurements on a gold RDE was typically 0 to −1.1 V vs SCE. For solutions A and B these measurements did not reveal anything above the residual current in the cathodic branch. Hydrogen evolution begins at about −0.75 V and its current is about 50% higher in solution B. It was also observed that current depended on the scan rate, however, there were no changes for scan rates higher than $10\,mV\,s^{-1}$. Even doubling the concentration of nickel in solution B, thus raising it to about 56% of the molar concentration of gold in solution D, did not reveal any changes. It indicates that hydrogen evolution reaction is easier than the nickel reduction in this solution.

After saturation of solution B with pure oxygen, one could observe oxygen reduction wave with $E_{1/2}$ about −0.35 V. After 5 min its current was about 4 μA, after 10 min about 8 μA and no further increase was observed. After a further 2 h of purging with nitrogen, the current in this region remained below 1 μA, which is in excellent agreement with its value prior to the saturation.

In solutions C and D the following phenomena were observed:

(i) The shape of the LSV curves, measured on a RDE, depended on scan rate. The set of curves reflecting this dependency is shown in Fig. 1; for higher scan rates ($> 50\,mV\,s^{-1}$) the curves in a set measured at different rotation rates remained the same within the experimental error.

(ii) Using our bath performance checking procedure,

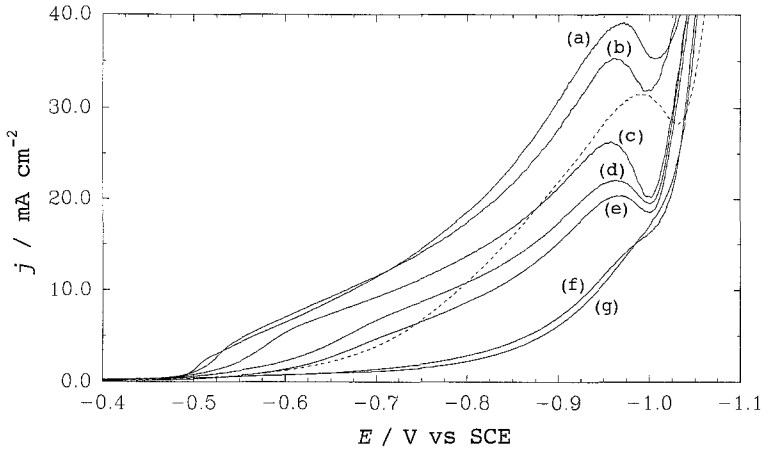

Fig. 1. Dependence of the shape of LSV curves on scan rate in solution C (soft gold) at rotation rate 2600 rpm. Curves correspond to following scan rates: (a) 1, (b) 2, (c) 5, (d) 10, (e) 20, (f) 50 and (g) 100 mV s^{-1}. Curve represented by a dotted line was determined before the 'activation' of the bath (actual scan rate 20 mV s^{-1}).

it was observed that the first (sometimes also, to a lesser extent, the second) curve taken either in a fresh solution C or D differed significantly from the others; such an example for $v = 20\,\text{mV s}^{-1}$ is shown in Fig. 1. It was found that repeating the measurement once or twice always removed this discrepancy. It was also possible to replace these additional measurements by simple galvanostatic electrolysis in the solution. The minimum charge necessary to achieve the effect was on the order of $4\,\text{mC dm}^{-3}$ of solution with current density at least $0.125\,\text{mA cm}^{-2}$. These observations indicate that this effect is due to some, yet unidentified, reactions in the solution causing an effect of bath 'activation';

On the basis of the above described experiments, we have selected a standard set of conditions for further studies of solutions C and D. Fifteen rotation speeds were used in the range 200 to 4000 rpm and the sweep rates were 1 and 20 mV s^{-1}; for the sweep rates above 20 mV s^{-1} no differences were observed between LSV curves.

3.2. *LSV experiments*

A set of LSV curves obtained in solution C is shown in Fig. 2 at $v = 1\,\text{mV s}^{-1}$ (a, b) and at $v = 20\,\text{mV s}^{-1}$ (c, d), and those in solution D in Fig. 3 at $v = 1\,\text{mV s}^{-1}$ (a, b) and $v = 20\,\text{mV s}^{-1}$ (c, d). A peak, probably associated with the inhibition due to the production of poison on the electrode surface (see Section 4), followed by a minimum is observed on LSV recorded at lower scan rates in solutions C and D. The shape of the voltammetric curves allows us to conclude that there are apparently two distinct mechanisms for gold deposition occurring in the potential range studied. These curves also reveal a strong inhibiting influence of nickel on gold plating as lower current densities are observed in solution D. It is also worth noting that the minimum on LSV is shifted towards more positive potentials when moving from solution C to solution D (soft to hard gold plating).

Acquired data were tested according to the Levich equation: $j_d = A\omega^{1/2}$, describing the diffusional character of the current (ω denotes the angular velocity, A is a constant) and also against the relation $1/j = 1/j_k + 1/j_d$, where j_k and j_d denote kinetic and diffusional contributions to the observed current, respectively. Plots of j against $\omega^{1/2}$ for solution C at $v = 1\,\text{mV s}^{-1}$ are shown in Fig. 4. One can conclude that the process remains under kinetic control (almost horizontal lines) in the potential range −0.5 to −0.6 V, with diffusional contribution increasing when moving towards more negative potentials.

Figure 5 displays examples of $1/j$ against $\omega^{-1/2}$ plots for solution C at $v = 1\,\text{mV s}^{-1}$. The resulting series of intercepts is a basis for the final plot in Fig. 6(a), where logarithmic dependence of the kinetic current density j_k on potential permits determination of Tafel slope, as equal to $-0.39\,\text{V dec.}^{-1}$ at potentials between −0.5 to −0.95 V. Figure 7 shows the plots of j against $\omega^{1/2}$ and $1/j$ against $\omega^{-1/2}$ for solution D at $V = 1\,\text{mV s}^{-1}$. It should be added that such procedure was possible only in the case of solution C at $v = 1\,\text{mV s}^{-1}$ and for solution D over a very narrow potential range. Tafel slopes could not be determined by this method at potentials more negative than the LSV maxima due to the inhibition effect.

We have calculated, on the basis of Levich equation, the limiting current density for the laboratory experiments on the gold RDE at 2700 rpm as approximately equal to $0.09\,\text{A cm}^{-2}$ and the linear velocity at RDE surface equal to $1.25\,\text{cm s}^{-1}$. During a typical industrial jet plating process, the corresponding linear velocities are 400–500 cm s^{-1}, leading to much larger limiting currents (2–4 A cm^{-2} on the basis of the wall-jet electrode theory [68]). The comparison of the current densities used in practical applications with the limiting current values allows us to conclude that the industrial process is kept well below the limiting current.

3.3. *Chronoamperometric and chronopotentiometric experiments*

Figure 8(a) displays a set of several chronoamperometric transients on the gold RDE at selected potentials (full set contained data from −0.40 to −1.10 V measured in 25 mV increments for each rotation rate). The initial sharp decrease of current cannot be ascribed exclusively to the double layer charging. The charge is too large and the corresponding time too long. At more negative potentials, particularly in

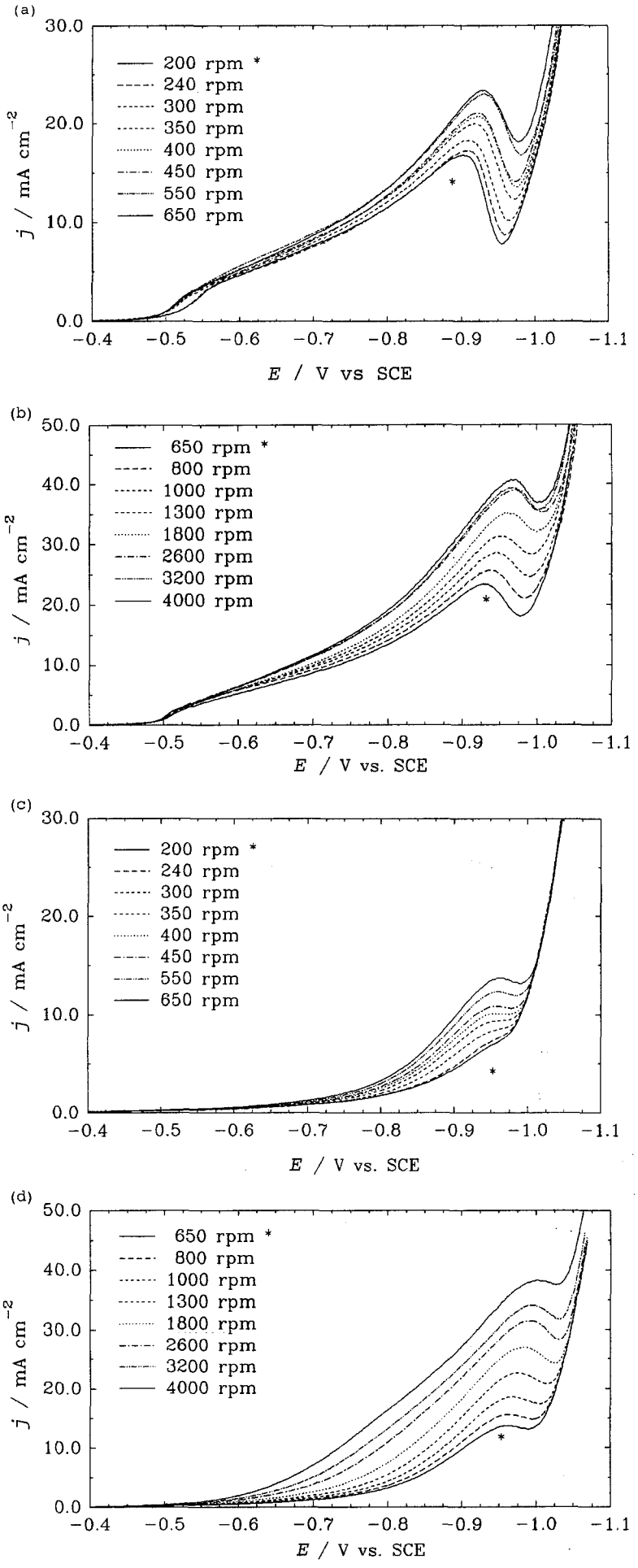

Fig. 2. LSV curves in solution C at 1 mV s^{-1} (a, b) and at 20 mV s^{-1} (c, d). Rotation rates (from bottom curve to top, respectively): (a and c) 200, 240, 300, 350, 400, 450, 550 and 650 rpm; (b and d) 650, 800, 1000, 1300, 1800, 2600, 3200 and 4000 rpm.

solution D, one can observe a maximum directly after the minimum, followed by a clear plateau, Fig. 8(a). In Fig. 8(b), examples of chronopotentiometric curves are displayed. They are characterized by a maximum followed by a plateau. Figure 6(a) and (b) (solution C) and Fig. 9(a) and (b) (solution D) present corresponding Tafel plots obtained from the galvanostatic and potentiostatic experiments. These plots were based on the potential maxima in the galvanostatic (Fig. 9(a)) and current minima, maxima and plateau in the potentiostatic (Fig. 9(b)) and experiments, at the largest rotation rate of 4000 rpm. The plot in Fig. 9(c) was obtained from the chronoamperometric experiments determined at various rotation rates with subsequent determination of the kinetic current from the intercept of the relation of j against $\omega^{-1/2}$. Plots in Fig. 9 reveal two slopes for two potential ranges, higher at more positive and lower at more negative potentials.

Average values of Tafel slopes, determined in different plating solutions and by different experimental techniques, are collected in Table 1. From these results, the following may be concluded:

(i) Tafel slopes obtained by the potentiostatic technique are in a good agreement with those obtained by the galvanostatic one, indicating that both techniques may be, in principle, used for the determination of Tafel parameters.
(ii) Tafel slopes obtained in solution D are higher than those in solution C indicating the influence of nickel on gold deposition.
(iii) Tafel slopes at more positive potentials are larger than those at more negative potentials.
(iv) There is no large difference between Tafel slopes estimated at 4000 rpm and on the basis of the kinetic current (from $1/j$ against $\omega^{-1/2}$). This is caused by relatively flat dependence of $1/j$ against $\omega^{-1/2}$ and it constitutes an additional proof of kinetic limitation of the process. This can also justify use of single series of measurements only at high rotation rate, as far less time and labour consuming procedure than the extrapolation.

3.4. *Determination of current efficiencies*

The measurements of current efficiencies have been carried out mainly in the galvanostatic mode and without deoxygenation, to bring the conditions closer to those in the industrial process. The platinum RDE was plated under different conditions and subsequently, the gold layer was stripped off galvanostatically in 1 M HCl with a current density of $20\,mA\,cm^{-2}$. We have also tried to determine the amount of deposited gold on the basis of stripping data, but because a mixture of Au(I) and Au(III) was obtained, its stoichiometry was not well defined. Hence, the final determination was then carried out by means of AAS. The results are summarized in Tables 2 and 3. It should be mentioned that a charge of 480 mC results in 0.56 μm deposit thickness (desired thickness) assuming 100% current efficiency.

The results obtained show that the average value of number of electrons, n, equals 1.72 with the relative standard deviation (RSD) 5.9%. Relative standard deviation of AAS determinations was much lower, therefore, we decided to rely on the direct AAS determination of amount of gold deposited.

Study of the dependence of current efficiency on current density at constant charge (i.e., 480 and 1600 mC, respectively) and without any special preparation of platinum surface before plating was carried out. In these experiments platinum RDE had been polished once, before the beginning of these measurements and it was washed with deionized water before electrodeposition and after each stripping. Data in Table 2 shows that for low deposition charge, there is a small, but clearly marked increase in current efficiency with increase in current density. This may be explained by the fact, that hydrogen evolution, which is undoubtfully the competitive reaction, occurs more easily on platinum than on gold and the time of exposition of the former is longer at low current densities. In this series colour of the deposits varied with current density: for the smallest value the deposits were orange and dull, becoming more pale with its increase, finally bright and light yellow with a touch of green. However, for relatively high charge passed (1600 mC), current efficiency decreases with increase of current density and increases with increase of the rotation speed. Deposits in this series were turning darker for current densities above $200\,mA\,cm^{-2}$ and some black spots could be observed for 600 and $800\,mA\,cm^{-2}$.

For constant plating current density ($100\,mA\,cm^{-2}$), current efficiency seems to increase with deposition charge at lower charges, while it is unchanged at higher charges (Table 2). In spite of varying charge, the RSD of the results in this Table is only 3.4%. In this series all the deposits were bright and light yellow, with a touch of green.

To check ambiguities concerning stripping data, we tried to prepare the electrode surface before plating by performing hydrogen evolution reaction in 1 M H_2SO_4 with current density $j_R = 20\,mA\,cm^{-2}$ for 5 min. There is the same trend as in the earlier series, the values of current efficiency, however, seem to be a little higher. To check this supposition, we have performed two additional series of measurements. All measurements in both series were carried out under identical conditions, ($j = 100\,mA\,cm^{-2}$, plating charge $Q_{DEP} = 500\,mC$) the sole difference between them was that, in the first series, there was no special preparation of the platinum surface before plating, whereas, in the second series, the electrode was treated prior to each determination that the surface was reduced in 1 M H_2SO_4 at $j_R = 20\,mA\,cm^{-2}$ for 5 min.

The RSD of the current efficiencies are very small and the confidence intervals below 1% (for confidence level 95%) in both series. The scattering of results is slightly higher for the reduced electrodes, but

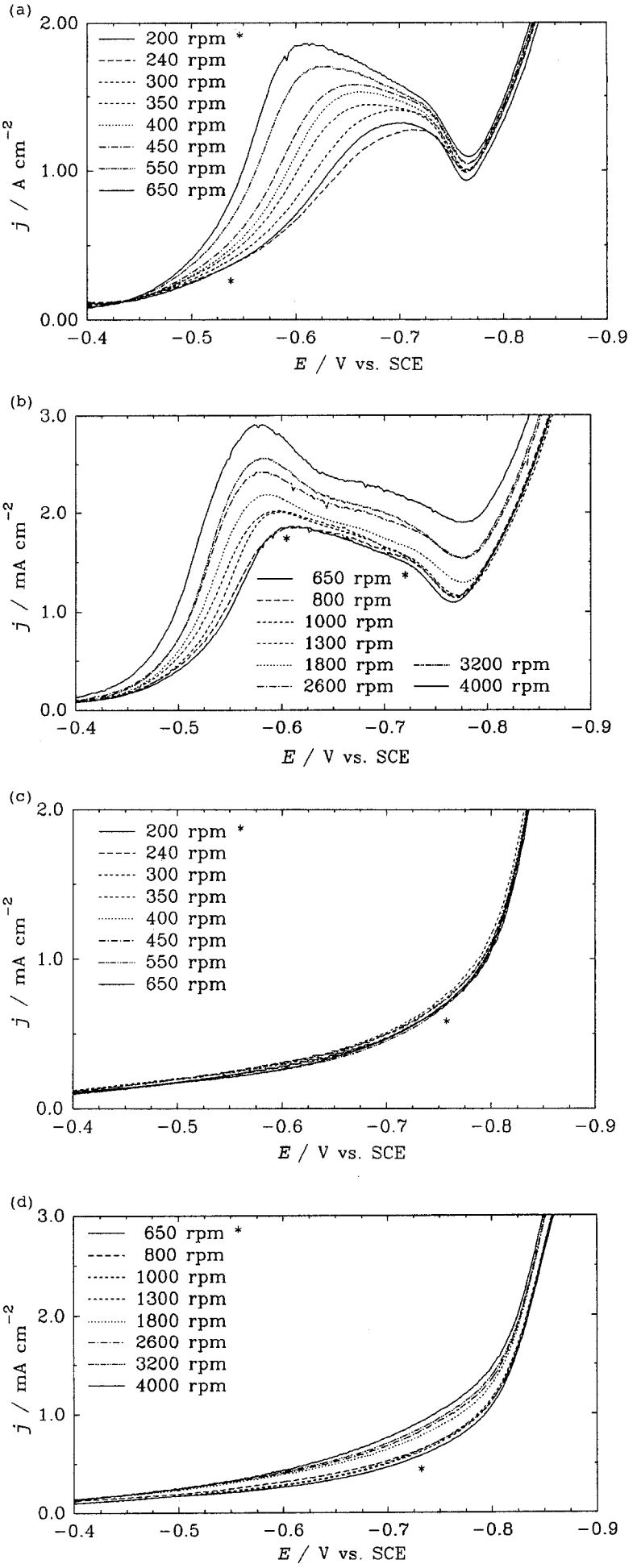

Fig. 3. LSV curves in solution D (hard gold) at 1 mV s^{-1} (a, b) and at 20 mV s^{-1} (c, d). Rotation rates as for Fig. 2.

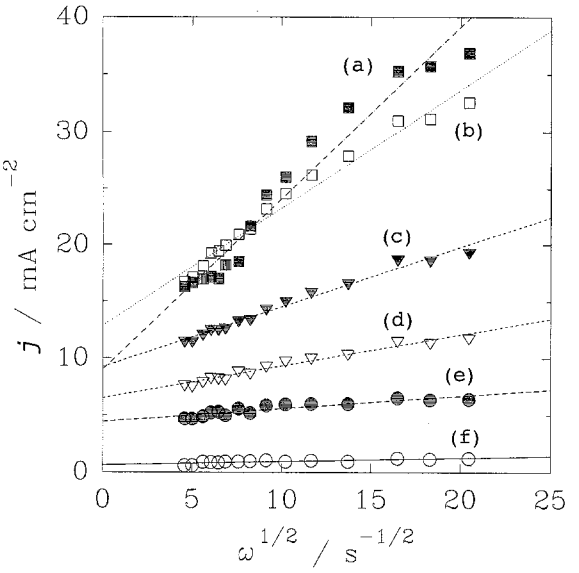

Fig. 4. Plots of j against $\omega^{1/2}$ constructed on the basis of the curves shown in Fig. 3 (a, b), i.e. solution C at 1 mV s^{-1}. (For clarity only selected curves are shown.) Curves: (a) −1.00, (b) −0.90, (c) −0.80, (d) −0.70, (e) −0.60 and (f) −0.50 V.

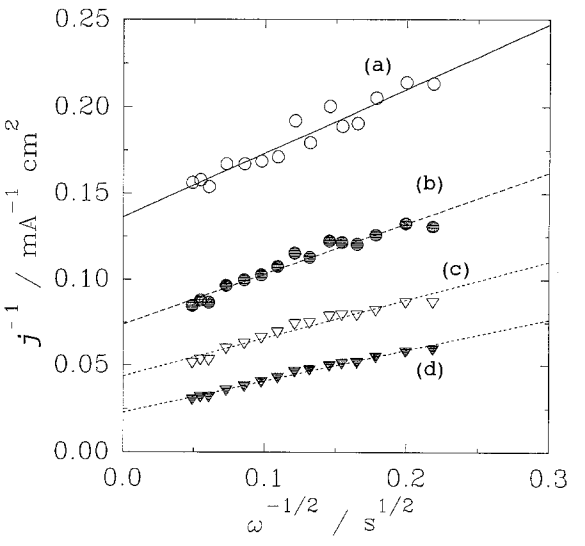

Fig. 5. Plots of $1/j$ against $\omega^{-1/2}$ constructed on the basis of the curves shown in Fig. 3 (a, b), i.e., solution C at 1 mV s^{-1}. (For clarity only selected curves are shown.) Curves: (a) −0.60 (b) −0.70, (c) −0.80 and (d) −0.90 V.

comparison of the precision of both series by means of the F-Snedecor test allows us to claim that there are no statistically significant differences between the two series at confidence level of 95% (RSD of the average: 0.81 and 1.26 for two series), as the calculated value of F parameter is much lower than its critical value ($F = 2.83 < F_{cr}(95\%, 4, 4) = 6.39$). The t-Student test reveals a significant statistical difference between the means, both on the 95% and even 99% confidence levels ($t = 10.97 > t_{cr}(99\%, 8) = 2.90 > t_{cr}(95\%, 8) = 1.86$). This tells that the state of the platinum surface is essential for deposition, even for high charges, because it affects current efficiency.

Comparison of two other series of measurements, with and without deoxygenation, indicates that the deaeration does not influence the results. With a difference between the average values of the two series equal to 1.5%, neither the F-Snedecor test revealed any significant statistical difference in precision ($F = 3.42 < F_{cr}(95\%, 4, 4) = 6.39$), nor the t-Student test between the two averages ($t = 1.22 < t_{cr}(95\%, 8) = 2.306$). Therefore, it is obvious that oxygen reduction plays a minor role in the overall process.

We have also performed measurements of current efficiency in a potentiostatic mode. The results are summarized in Table 3. The purpose of this experiment was to provide data concerning hydrogen evolution and to allow necessary corrections before the attempts at computer simulation of nucleation and crystal growth. For these purposes, the curves measured on the gold RDE were selected and charges calculated (taking into account the difference in areas of both RDEs) for the platinum RDE, in order to stop the experiment at a given preselected point of the curve (e.g., in the initial 'well' or on the final plateau). However, the shape of the resulting potentiostatic transients on platinum was quite different than on gold, even for significant thickness of the deposit. Figure 10 demonstrates several potentiostatic deposition curves on both gold and platinum RDE at potentials of −0.5 and −0.7 V. Hence, the conclusions are of limited usefulness for the planned purposes. The results, shown in Table 3, can only reflect the fact that there is a maximum of current efficiency at −0.7 V, corresponding to the maximum on the LSV curves. Notice also that the optimum current efficiency does not lay at the very negative potential region, but of course 'overall' speed of plating is higher in that region due to a very big increase in total current (even if current efficiency is smaller by 20%). The quality of plating provides another argument for more negative potentials and higher current densities.

4. Conclusions

The following summary can now be given:

(i) The bath under study requires a certain charge to be passed to obtain optimum performance. In laboratory experiments, reproducible results could be achieved but only after several curves have been recorded, or an equivalent charge passed through the solution in a galvanostatic mode. In these experiments, a minimum value of charge was found to be 4 mC dm^{-3} and a minimum current density of about 0.125 mA cm^{-2}.

(ii) The oxygen dissolved in the solution did not have any important influence on current efficiencies.

(iii) The LSVs recorded on a RDE in Renovel bath indicate that soft and hard gold electrodeposition is controlled by the interfacial kinetics. There was no diffusion limited plateau in Figs. 1–3, contrary to the deposition in oxalate–phosphate [33] or cyanide [37] baths. Importance of the electrocrystallization kinetics is also evident from the potentiostatic and galvanostatic transients in Figs 8 and 10.

(iv) The LSV experiments also revealed a strong inhibiting influence of nickel on gold electrodeposition. Current densities are much lower for hard

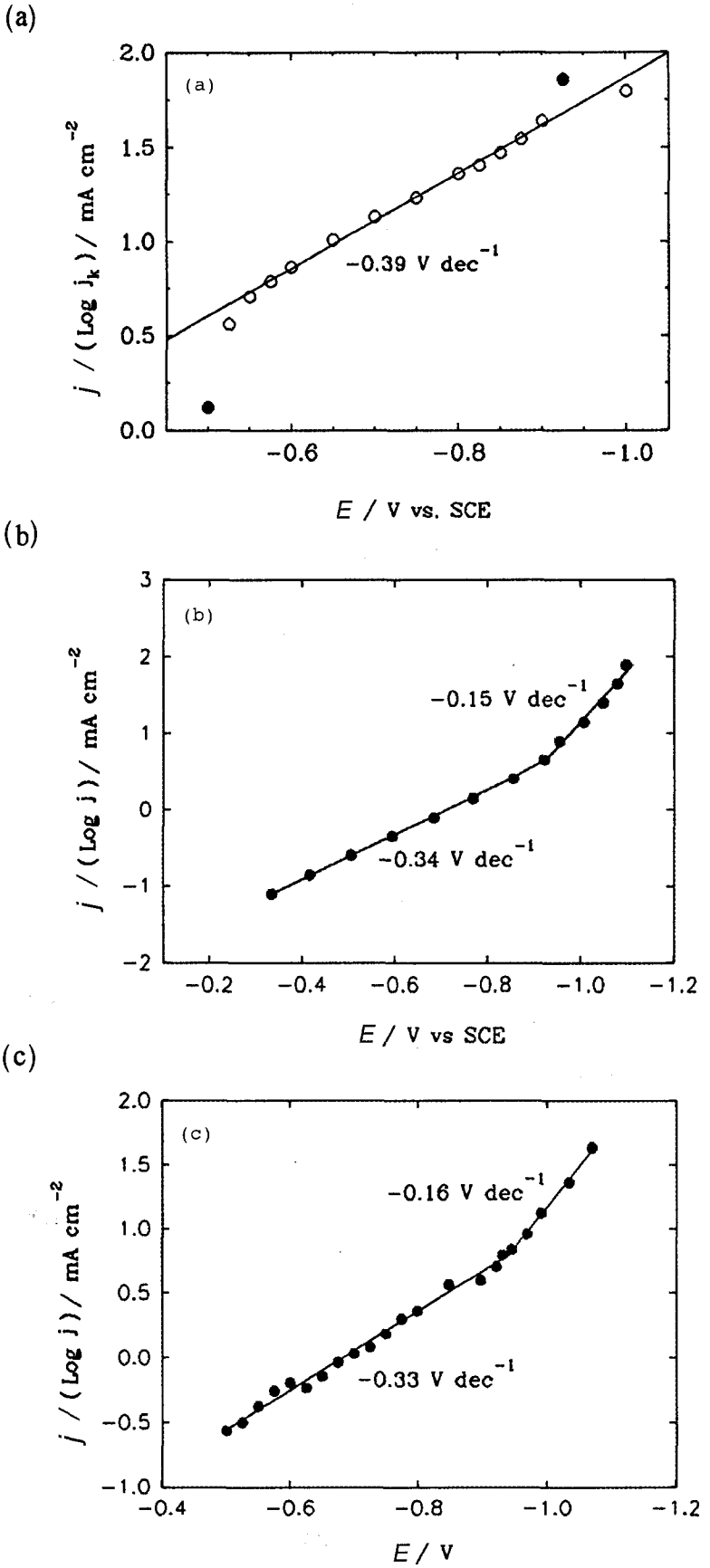

Fig. 6. Tafel plots constructed on the basis of (a) the kinetic current density (from extrapolation of $1/j$ against $\omega^{-1/2}$ in LSV experiments) for solution C at $1\,mV\,s^{-1}$ (points marked with filled symbols were not used in calculation of the slope); (b) the initial potential maxima on galvanostatic potential transients at 4000 rpm; (c) the initial current minima on potentiostatic current transients at 4000 rpm.

(solution D) as compared with soft (solution C) gold deposition. In the latter, the process remains under kinetic control down to −0.6 V, with diffusional contribution increasing at more negative potentials. In solution D diffusion seems to play a more important role.

(v) Comparison of the Tafel parameters collected in Table 1 indicates that in soft and hard gold plating

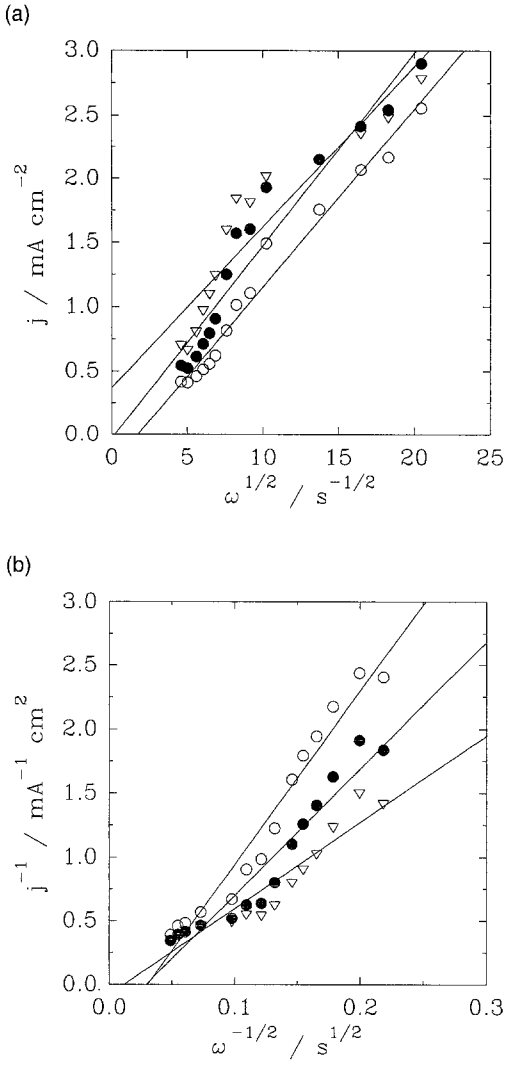

Fig. 7. Plots of j against $\omega^{1/2}$ and $1/j$ against $\omega^{-1/2}$ constructed on the basis of LSV curves in solution D (hard gold). Curves: (○) −0.550, (●) −0.575 and (▽) −0.600 V.

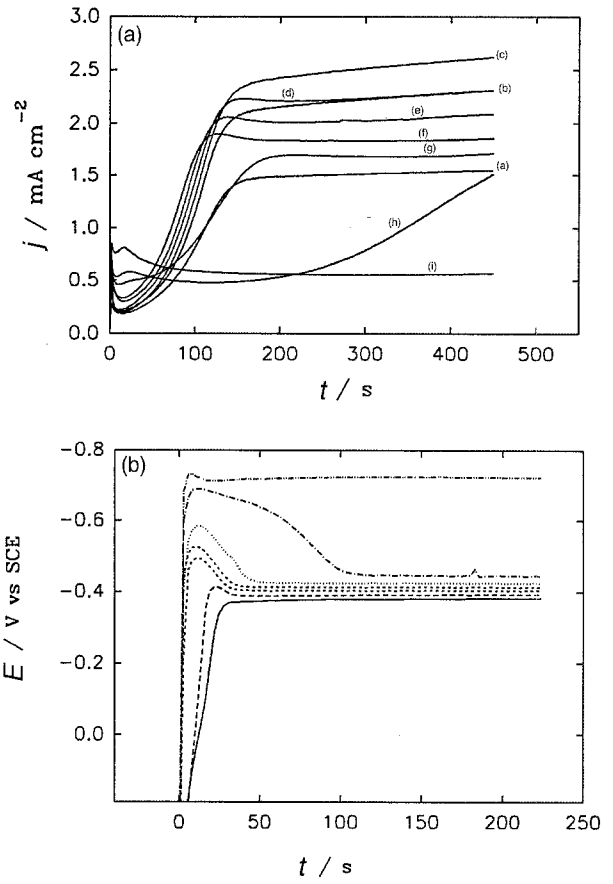

Fig. 8. Examples of chronoamperometric (a) and chronopotentiometric (b) transients obtained in solution D at the rotation rate of 4000 rpm. Curves for (a): (a) −500, (b) −525, (c) −550, (d) −575, (e) −600, (f) −650, (g) −700, (h) −725 and (i) −750 mV. Curves (bottom to top) for (b): 0.110, 0.170, 0.255, 0.354, 0.453, 0.623 and 0.792 mA cm^{-2}.

solution two different slopes were obtained. Similar results were obtained by chronoamperometric and chronopotentiometric techniques. In solution C (soft gold), a single Tafel slope at potentials more positive than the peak potential could be obtained from LSV measurements because of the inhibition of the process (decrease of the current after peak). The observed differences may be connected with the kinetics of gold nucleation and crystal growth, which is different in these two techniques. In LSV experiments nucleation begins gradually at more positive potentials and then the rate of crystal growth and nucleation accelerates as potential becomes more negative, whereas potential or current is kept constant in the other techniques. Moreover, time after which the measurements are made is different in LSV and other experiments.

(vi) Comparison of our results with those obtained by Bindra *et al.* [33] in weakly acidic oxalate–phosphate baths allows us to conclude that a similar mechanism of gold plating was observed in both cases. Bindra *et al.* obtained two distinct slopes of Tafel curves equal to −0.315 V dec.$^{-1}$ between −0.5

Table 1. Tafel slopes obtained in different plating solutions (C – soft gold, D – hard gold, 60 °C) and by chronoamperometry (CA), chronopotentiometry (CP) and linear sweep voltammetry (LSV)

Plating solutions	*Average Tafel slopes*/V dec.$^{-1}$		*Remarks*
	Range I	*Range II*	
C	−0.39 ± 0.01	−0.39 ± 0.01	Range: −0.50 to −0.95 V LSV method
	−0.35 ± 0.02	−0.154 ± 0.005	Range I: −0.50 to −0.95 V Range II: −0.95 to −1.1 V CA and CP methods
D	−0.47 ± 0.03	−0.186 ± 0.009	Range I: −0.50 to −0.80 V Range II: −0.80 to −1.1 V CA and CP methods

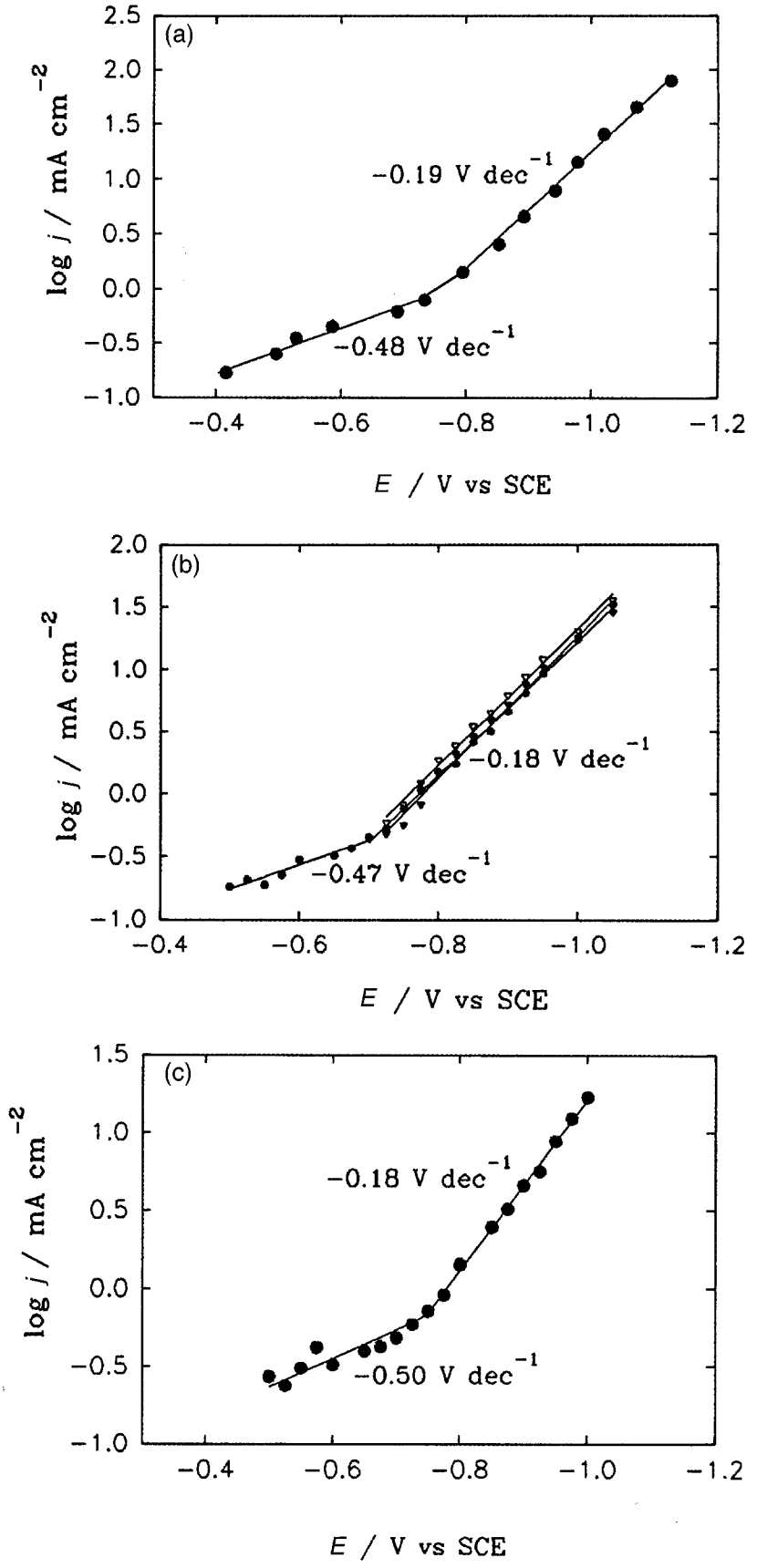

Fig. 9. Tafel plots, obtained in solution D: (a) on the basis of the initial potential maxima on galvanostatic transients at 4000 rpm, (b) based on current minima (●), maxima (▽) and plateaux (▼) on the potentiostatic current transients at 4000 rpm and (c) based on kinetic current density after extrapolation from $1/j$ against $\omega^{-1/2}$ relation from current density minima obtained from potentiostatic measurements.

and −0.8 V and −0.110 V dec.$^{-1}$ between −0.8 and −1.2 V for soft gold plating but only one slope of −0.200 V dec.$^{-1}$ between −0.3 and −0.7 V for hard gold plating. It is well established that gold deposition from cyanide complexes proceeds in two steps [33, 37], at more positive potentials through an adsorption stage:

$$Au(CN)_2^- \longrightarrow (AuCN)_{ads} + CN^-$$

Table 2. Current efficiencies for hard gold plating, solution D, temperature 60 °C, no deoxygenation, Pt RDE surface area 1 cm², rotation rate 2700 rpm, no special preparation of Pt surface before plating

j/mA cm^{-2}	Q_{DEP}/mC	Q_{SRT}/mC	m_{AAS}/mg	CE_{AAS}/%	n
10	481	336	0.433	44.1	1.58
20	484	358	0.444	44.9	1.65
40	488	415	0.453	45.5	1.87
60	546	435	0.544	48.8	1.63
80	484	403	0.503	50.9	1.64
100	487	459	0.539	54.2	1.74
100	1600		1.880	57.57	
200	1600		1.775	53.74	
400	1600		1.000	30.62	
600	1600		0.648	19.86	
600*	1600		0.846	25.90	
800	1600		0.518	15.86	
800*	1600		0.667	20.42	
100	100		0.095	46.54	
100	200		0.203	49.73	
100	300		0.296	48.34	
100	400		0.422	51.59	
100	500		0.561	54.97	
100	487	459	0.539	54.2	1.74
100	725	704	0.861	58.2	1.67
100	987	916	1.108	55.0	1.69
100	1300	1208	1.524	57.4	1.62
100	1465	1320	1.615	54.0	1.67

* rotation rate 4000 rpm.

Symbols used: Q_{DEP} and Q_{STR} charges of deposition and stripping, m_{AAS} and CE_{AAS} mass of gold and current efficiency determined by AAS, n average number of electrons per one Au atom during anodic stripping process.

$$(AuCN)_{ads} + e^- \longrightarrow (AuCN^-)_{ads}$$

$$(AuCN^-)_{ads} + H^+ \longrightarrow Au + HCN$$

whereas, at more negative potentials, direct electroreduction of the gold complex takes place:

$$Au(CN)_2^- + e^- + 2H^+ \longrightarrow Au + 2HCN$$

The reduction through adsorbed state leads to higher Tafel slopes. It must also be stressed, that nickel concentrations in the work of Bindra *et al.* were about two orders of magnitude lower than the corresponding concentrations in our work. Higher values of Tafel slopes and lower values of currents obtained in our experiments indicate stronger inhibition of the process by adsorption and greater influence of the electrocrystallization on the deposition kinetics. A small change in the slope of $1/j$ against $\omega^{-1/2}$ curves (Fig. 5) with the electrode potential was observed. This was similar to the results of Bindra *et al.* [33]. This change may be connected with a competition between the reduction of AuCN film and $Au(CN)_2^-$ complex from the solution.

Table 3. Current efficiencies for hard gold plating, solution D, conditions as in Table 2, Pt RDE surface reduced before each deposition in 1 M H_2SO_4, $j_R = 20\,mA\,cm^{-2}$, $t = 5\,min$

E_{DEP}/V	t_{DEP}/s	Q_{DEP}/mC	m_{AAS}/mg	CE_{AAS}/%
−0.500	200	362.3	0.464	62.74
−0.500	350	669.4	0.846	61.92
−0.700	130	386.1	0.573	72.71
−0.700	270	846.1	1.181	63.38
−0.900	100	445.3	0.498	54.79
−1.100	12	288.7	0.301	51.08

Symbols: E_{DEP} deposition potential against SCE, t_{DEP} deposition time.

Formation of a minimum on LSV (Figs 2 and 3) and decrease in plateau current on chronoamperometric curves (Fig. 8(a)) with increase of the negative potential indicates an autoinhibition process. The peak on the LSV curves increases with the increase in the rotation rate, and it is completely inhibited in the absence of rotation, thus indicating its dependence on the diffusion of an inhibitor. The inhibition might be caused by the cyanide species (CN^- or HCN) produced at the electrode surface and removed faster at higher rotation rates.

(vii) The lack of dependency of current efficiency on deposition charge remains in agreement with the results of Eisenmann [37], who also found a linear dependency between the amount of deposited gold and the plating time in the case of hard gold baths.

The coulombic efficiency of the process increases in the potential range −0.5 to −0.7 V from 51 to 73% and then decreases gradually as hydrogen evolution rate increases. It remains relatively constant at the range of −1.1 to −1.3 V (~55%). It must be stressed that a statistically significant difference was found in current efficiencies determined on the platinum RDE with its pretreatment by reduction in sulphuric acid

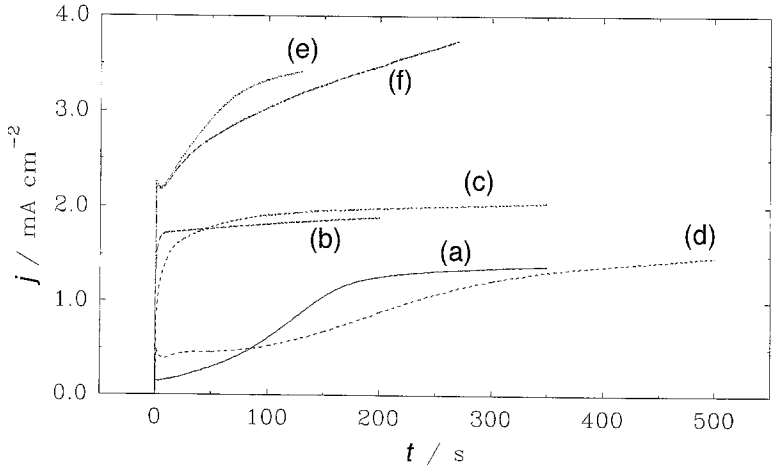

Fig. 10. Potentiostatic current transients on Au and Pt RDEs in solution D at rotation rate 2700 rpm after deposition of different charges of hard gold. Curves: (a) Au, −0.500 V against SCE; (b) Pt, −0.500 V against SCE, 362 mC cm^{-2}; (c) Pt, −0.500 V against SCE, 669 mC cm^{-2}; (d) Au, −0.700 V against SCE; (e) Pt, −0.700 V against SCE, 386 mC cm^{-2}; (f) Pt, −0.700 V against SCE, 846 mC cm^{-2}.

solution as compared with determinations on untreated surface. In the former case the value of current efficiency was about 8% (rel.) higher.

(ix) Slightly higher Tafel slopes were obtained for hard gold as compared with soft gold bath, and the currents observed in solution D were smaller. This indicates a strong influence of nickel on the gold electrocrystallization and stresses the importance of keeping the nickel concentration under control. A deeper insight in the role of nickel may be achieved by analysis of potentiostatic current transients on the basis of the theory of nucleation and crystal growth processes. These results will be presented in future papers.

Acknowledgements

Financial support from NSERC is gratefully acknowledged.

References

[1] F. H. Reid and W. Goldie (eds.), 'Gold Plating Technology', Electrochemical Publications, Ayr (1974).
[2] F. R. Schlodder, H. H. Beyer and W. G. Zilskie, 'GOLD 100', Proceedings of the International Conference on Gold, Johannesburg (1986) vol. 3, p. 21.
[3] E. A. Parker, *Plating* **45** (1958) 631.
[4] W. T. Lee, *Corros. Technol.* **10** (1963) 59.
[5] N. N. Balashova, T. A. Smirnova, N. A. Smagunova and A. K. Yudina, *Zh. Prikl. Khim.* **50** (1977) 2698.
[6] H. Angerer and N. Ibl, *J. App. Electrochem.* **9** (1979) 219.
[7] V. A. Zabludovskii, A. V. Krapivnoi, V. I. Kaptanovskii and N. A. Kostin, *Elektrokhimiya* **25** (1989) 1258.
[8] H. U. Galgon, *Feingerätetechnik* **38** (1989) 353.
[9] H. R. Khan, M. Baugärtner and Ch. J. Raub, Proceedings of the Symposium on Electrodeposition Technology: Theory and Practice, Electrochemical Society, Pennington NJ (1987) p. 165.
[10] H. L. Cohen, K. W. West and M. Antler, *J. Electrochem. Soc.* **124** (1977) 342.
[11] S. J. Hemsley and R. V. Green, *Trans. Inst. Metal Finish.* **69** (1991) 149.
[12] L. Sjögren, B. Asthner, L-G. Liljestrand and L. B. Révay, *Plat. Surf. Finish.* **73** (1986) 70.
[13] H. Leidheiser Jr., A. Vértes, M. L. Varsányi and I. Czakó-Nagy, *J. Electrochem. Soc.* **126** (1979) 391.
[14] A. Knödler, *Galvanotechnik* **68** (1977) 383.
[15] R. M. Krishnan, S. Sriveeraraghavan and S. R. Natarajan, *Met. Finish.* **86** (1988) 56.
[16] J. M. Leeds and M. Clarke, *Trans. Inst. Met. Finish* **47** (1969) 163.
[17] R. L. Cohen, F. B. Koch, L. N. Schoenberg and K. W. West, *J. Electrochem. Soc.* **126** (1979) 1608.
[18] V. A. Zabludovskii, A. V. Krapivnoi, V. I. Kaptanovskii, N. A. Kostin, I. Z. Gubaidulin and A. M. Avidon, *Zashchita Metallov* **23** (1987) 1038.
[19] L. Holt, R. J. Ellis and J. Stanyer, *Plating* **60** (1973) 918.
[20] V. N. Fedorova and B. S. Krasikov, *Zhur. Prikl. Khimii* **50** (1977) 792.
[21] J. Socha, E. Raub and A. Knödler, *Metalloberfläche – Angewandte Elektrochemie* **26** (1972) 125.
[22] J. Socha, E. Raub and A. Knödler, *ibid.* **27** (1973) 1.
[23] E. Raub, S. Pahlke and H. P. Wiehl, *Metalllwiss. u. Techn.* **25** (1971) 735.
[24] B. Inglot, J. Socha, A. Pęziński, *Powłoki ochronne* **9** (1981) 31.
[25] J. Socha, T. Żak, *Prace Inst. Mech. Prec.* **14** (1966) 1.
[26] K. J. Whitlaw, J. W. Souter, I. S. Wright and M. C. Nottingham, *IEEE Trans. Comp. Hybr. Manufact. Technol.* **8** (1985) 46.
[27] H. A. Reinheimer, *J. Electrochem. Soc.* **121** (1974) 490.
[28] F. B. Koch, Y. Okinaka, C. Wolowodiuk and D. R. Blessington, *Plat. Surf. Finish.* **67** (1980) 50.
[29] F. B. Koch, Y. Okinaka, C. Wolowodiuk and D. R. Blessington, *ibid.* **67** (1980) 43.
[30] S. Nakahara and Y. Okinaka, *J. Electrochem. Soc.* **128** (1981) 284.
[31] K. Lin, R. Weil and K. Desai, *ibid.* **133** (1986) 690.
[32] D. W. Endicott and G. J. Casey Jr., *Plat. Surf. Finish.* **67** (1980) 58.
[33] P. Bindra, D. Light, P. Freudenthal and D. Smith, *J. Electrochem. Soc.* **136** (1989) 3616.
[34] B. Vincent, P. Bercot, G. F. Creusat, G. Messin and J. Pagetti, *Plat. Surf. Finish.* **77** (1990) 71.
[35] G. Holmbom and B. E. Jacobson, *J. Electrochem. Soc.* **135** (1988) 2720.
[36] Ch. J. Raub, H. R. Khan and M. Baumgärtner, *Gold. Bull.* **19** (1986) 70.
[37] E. T. Eisenmann, *J. Electrochem. Soc.* **125** (1978) 717.
[38] M. Fleischmann and H. R. Thirsk, *in* 'Advances in Electrochemistry and Electrochemical Engineering' (edited by P. Delahay) Wiley Interscience, New York (1963) pp. 123–210.
[39] J. A. Harrison and H. R. Thirsk, *in* 'Electroanalytical Chemistry' (edited by A. J. Bard) vol. 5, Marcel Dekker, New York (1971) pp. 67–148.
[40] S. T. Rao and R. Weil, *Trans. Inst. Metal Finish.* **57** (1979) 97.
[41] D. Davidović and R. R. Adzić, *Electrochim. Acta* **33** (1988) 103.
[42] G. Scholze, S. Hunger and S. Skladnikiewitz, *Stahlberatung* **10** (1983) 4.
[43] J. A. Lochet, *WIPO Patent WO/88/09835* (1988).
[44] *Idem, US Patent 4 670 107* (1987).
[45] *Idem, US Patent 4 744 871* (1988).
[46] J. A. Lochet and R. B. Patel, *US Patent 4 755 264* (1988).
[47] J. A. Lochet, Proc. AESF Annu. Tech. Conf. 77th, (1990), vol. 2, pp. 983–1002.
[48] E. T. Eisenmann, *J. Electrochem. Soc.* **124** (1977) 1957.
[49] Y. Okinaka and C. Wolowodiuk, *ibid.* **128** (1981) 288.
[50] G. B. Munier, *Plating* **56** (1969) 1151.
[51] Y. Okinaka, F. B. Koch, C. Wolowodiuk and D. R. Blessington, *J. Electrochem. Soc.* **125** (1978) 1745.
[52] M. Antler, *Plating* **60** (1973) 468.
[53] D. Mason, *Plat. Surf. Finish.* **73** (1986) 14.
[54] A. Knödler, *Metalloberfläche – Angewandte Elektrochemie* **28** (1974) 465.
[55] L. Holt and J. Stanyer, *Trans. Inst. Metal Finish.* **50** (1972) 24.
[56] L. Holt, R. J. Ellis and J. Stanyer, *Plating.* **60** (1973) 910.
[57] H. A. Reinheimer, *J. Electrochem. Soc.* **121** (1974) 490.
[58] C. J. Raub, A. Knödler and J. Lendvay, *Plat. Surf. Finish.* **63** (1976) 35.
[59] Y. Okinaka, Proceedings of the Symposium on Electrodeposition Technology: Theory and Practice, Electrochemical Society, Pennington NJ (1987), p. 147.
[60] G. Holmbom and B. E. Jacobson, *J. Electrochem. Soc.* **135** (1988) 787.
[61] D. L. Malm and M. J. Vasile, *ibid.* **120** (1973) 1484.
[62] H. Graham Silver, *ibid.* **116** (1969) 591.
[63] L. Silverman, B. Bernauer and F. Pettinger, *Met. Finish.* **68** (1970) 48.
[64] Y. Okinaka and S. Nakahara, *J. Electrochem. Soc.* **123** (1976) 1284.
[65] R. Wiart, *Electrochim. Acta* **35** (1990) 1587.
[66] K.-L. Lin, W.-Ch. Liu, M. H. M. Lin and Y. W. Hu, *J. Electrochem. Soc.* **138** (1991) 3276.
[67] F. C. Walsh and D. R. Gabe, *Surf. Technol.* **12** (1981) 25.
[68] J. Yamada and H. Matsuda, *Electroanal. Chem. Interfacial Electrochem.* **44** (1973) 189.
[69] W. J. Albery and Ch. M. A. Brett, *J. Electroanal. Chem.* **148** (1983) 201.
[70] *Idem, ibid.* **148** (1983) 211.